# Analysis and imaging of the GTFs data from the eastern margin of the Bohemian Massif and the West Carpathians

Světlana Kováčiková, Václav Červ, Josef Pek and Oldřich Praus
Geophysical Institute, Acad. Sci. Czech Rep., Prague
Boční II/1401, CZ - 141 31 Prague 4-Spořilov, Czech Republic

**Abstract**

Geomagnetic variation data recorded during several field campaigns along profiles traversing the eastern margin of the Bohemian Massif and the West Carpathians extending over border territories of Poland and of the Czech and Slovak Republics were used to estimate geomagnetic transfer functions (GTFs) and the induction arrows for periods ranging from about 12 to 96 minutes. In order to get a deeper insight into the causative phenomena of the large-scale inductive anomalies observed within the area of investigations, the GFTs data set from 150 field sites was used to compute and map simulated anomalous magnetic fields across the region by separating the fields into external and internal parts and applying the hypothetical event analysis (HEA). A possible effect of static distortions on the GTFs is analyzed. Equivalent current systems in a thin sheet embedded at different depths in a two-layer medium are computed for the observed GTFs. Possible geological implications are considered.

## 1 Introduction

The West Carpathian conductivity anomaly (WCA) is a phenomenon known for more than twenty years. It represents a prominent inductive anomalous feature that distinctly delineates the contact zone between the West Carpathians (WCP), as a sub-unit of the Tertiary Alpine orogenic belt, and the surrounding older units, specifically the Bohemian Massif (BM) in the west and the Polish Paleozoic Platform in the north. In the east of the Bohemian Massif, this anomaly adjoins, or merges with the eastern termination of the whole Hercynian orogene, representing thus a zone of the first order significance with regard to the European tectonic structure and history. In spite of the enormous knowledge accumulated in this zone so far, the geological structure and evolution of the eastern margin of the Hercynides, including the transition zone between the Bohemian Massif and the Carpathians as a particular segment, is a problem still unresolved in detail.

Extensive geomagnetic induction investigations, carried out in the area of the transition zone between the BM and the WCP over almost thirty years, have resulted in collecting a large set of long period geomagnetic transfer functions (GTFs, period range from 1000 to about 7000 s) distributed uniformly across the whole of the target area. Besides the detailed delineation of the WCA along the whole Czech, Slovak and Polish segment of the Carpathian belt, the inductive pattern has clearly revealed that the BM-to-WCP transition cannot be considered a single contact, but that it rather represents a two-step process demarcated by the WCA in the east and by another regional inductive anomaly (BMA), about 100 km to the west of the WCA, which can be attributed to the eastern margin of the BM (Fig. 1).

Several studies so far published on the BMA area (Pěčová et al., 1976; Pícha et. al., 1984; Červ et al. 1984, 1987) have shown highly inhomogeneous distribution of the electrical conductivity in the transition zone between the BM and the WCP units and suggested two zones of anomalous induction at the eastern margin of the BM and near the boundary of the Outer and Central WCP (Praus and Pěčová 1991; Pěčová and Praus 1996). The papers addressed, in brief, two particular questions: (a) the detailed course of the anomaly, inferred from the spatial morphology of the geomagnetic transfer functions, and its formal relation to the underlying geological structures, and (b) a formal estimation of some source parameters for the BMA (depth to the conductor, conductance estimates), based mainly on 2-D theoretical concepts,

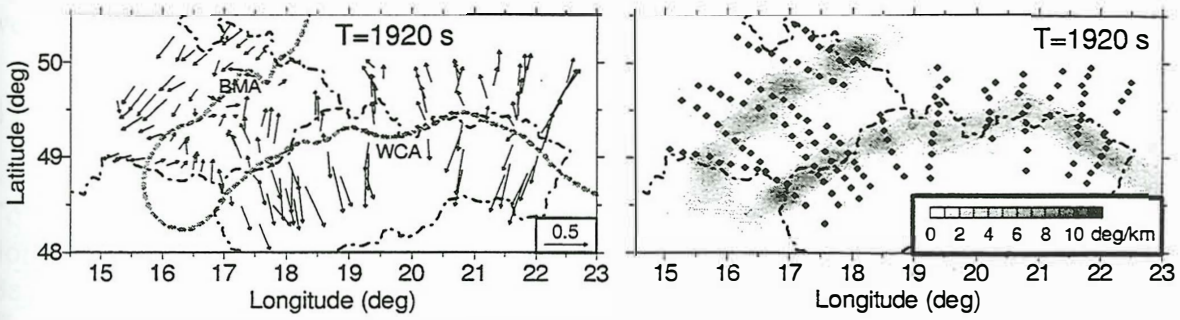


**Figure 1: Left** - Real induction arrows across the eastern margin of the Bohemian Massif and its transition to the West Carpathians for the period of 1920 s. The gray dashed line is the zero contour of the real N-component of the GTFs, which delineates the WCA and BMA induction anomalies in the best way. **Right** - Gray scale map of the module of the gradient of the azimuth of the real induction arrows across the area, which identifies the WCA and BMA anomalies as quasi-linear zones with the most rapid changes of the azimuth of the induction arrows. By diamonds, the measurement sites are marked.

evidently oversimplified in this case. The problem is that, unlike the WCA, which is an evident quasi-linear inductive feature within the crust manifested by clear reversals of strike-perpendicular induction arrows along its axis, the anomaly on the eastern margin of the Bohemian Massif has essentially a different character. As far as experimentaly documented, it is (i) a quasi-linear phenomenon, extending over more than 100 km in rougly the SW-NE direction, (ii) defined by a fast change of the azimuths of the induction arrows along its axis, but (iii) characterized, contrary to a 2-D setting, by large (sometimes, in fact, dominating) strike-parallel components of the induction arrows. The latter feature suggests that the BMA is strongly influenced by 3-D conductivity effects, either inductive or of a distortion nature. Due to the long periods involved, the observed distribution of the induction characteristics does not necessarily reflect only the local features of the conductivity distribution, but can be affected by induction processes taking part in structures either remote, or over-regional with respect to the particular area of interest. Therefore, as a first step in the search for the real 3-D conductivity conditions of the region, we have carried out a series of formal data imaging and transformation procedures, aiming at (i) estimating the degree of the 3-D distortions that affect the induction data in the BMA zone, (ii) determining the preferred directions of the causative currents for the BMA, and (iii) inferring possible regional configurations of the anomalous conductivity structures which can produce the induction pattern observed. In this paper, we present selected results of these imaging experiments and point out some correlations with the geological features of the region involved.

## 2 Geology, the experimental data

The region under investigation extends over the eastern margin of the Bohemian Massif (BM) and the West Carpathians (WCP) representing two fundamental elements of Europe that make contact here. The BM builds up Bohemia and the western part of Moravia and represents the easternmost consolidated part of the orogenic belt known as European Hercynides (Meso-Europe) extending across Europe from the Pyrenean peninsula to the Black sea. The determining element of the structure of the BM are several SW-NE trending zones separated usually by deep-seated faults, which are usually reflected very distinctly in the geophysical fields. The fault structures are essentially parallel with the boundaries of individual Hercynide zones. The intersection of these zones with the second order system of NW-SE trending faults is responsible for the complicated block structure of the BM. Those blocks in the east, northeast and

southeast margin of the BM related to the region of our investigations are the Moravian Moldanubicum, the Moravo-Silesian zone (Moravicum and Silesicum) and the Sudeticum.

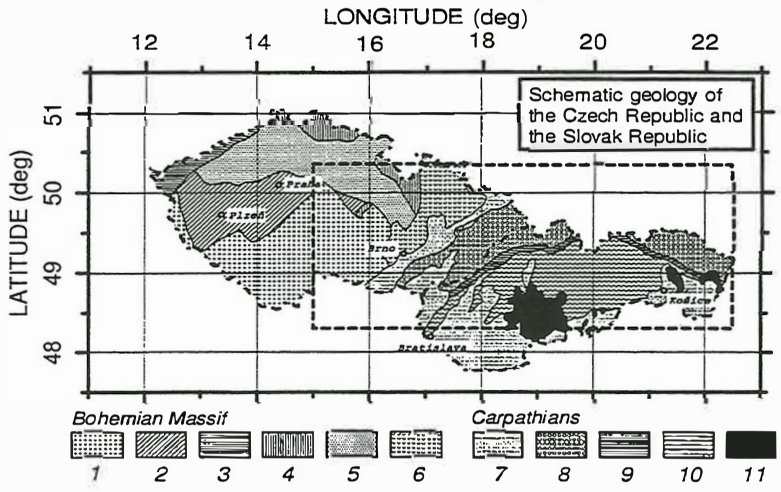


**Figure 2:** Geological structure of the Czech and Slovak Republics. **Bohemian Massif (BM) with units:** 1-Moldanubicum; 2-Teplá-Barrandian region; 3-Krušné hory-Thuringian region; 4-West-Sudetic region; 5-Bohemian Cretaceous basin; **Brunovistulicum (BV):** 6-Brunovistulicum including Silesicum, Moravicum and Brno Massif; **West Carpathians with units:** 7-Tertiary basins (Carpathian foredeep, Pannonian basin); 8-Outer (Flysch) Carpathians; 9-Klippen Belt; 10-Central (Inner) Carpathians; 11-Neovolcanites. Area bounded with thick dashed line marks the region of 150 field stations occupied during field experiments and with induction response data available from subsequent analysis.

The WCP belong to the young Tertiary Alpine orogenic belt and they constitute the northern branch of the Alpides. Their boundary with the Eastern Alps runs along the Danube Valley. The northern boundary with the East European Platform is defined by the erosive margin of flysch nappes. The WCP region is divided into several zones, each of which is characterised by its historical evolution and structure. Following zones are distinguished (i) the Inner (Central Carpathians), (ii) the Klippen zone, (iii) the Outer (Flysch) Carpathians and (iv) the Carpathian Foredeep.

There is the Brno unit or Brunovistulicum (BV) (original name Brno unit by Zapletal, 1932, or recently Brunovistulicum (BV) according to Dudek, 1980; Suk, 1995) in between those previously mentioned structural units. The BV is assumed to be an independent Cadomian geological unit forming the basement of the WCP in Moravia and the eastern part of the Hercynides (Variscides) of the BM. This unit seems to be linked with fundamental elements of the central European geological structure, specifically, with the Trans-European Suture Zone that represents the most important geological boundary in Europe separating mobile Phanerozoic western terranes (Meso-Europe) from the Precambrian east European Craton (Červ et al., 1997). According to recent investigation of the deep structure, geochronometric and geological information this unit probably belongs to the Fenno-Sarmatian (East-European) Platform (Weiss, 1977; Dudek, 1980; Mísař et al., 1983; Suk, 1995).

Field experiments in this area were organised to map systematically zones of anomalous induction and to understand their nature. The eastern margin of the BM, the whole Moravia and the WCP region were covered by a total of 150 temporary geomagnetic field stations, where $H_x$ (+ northward), $H_y$ (+ eastward), $H_z$ (+ downward) components were recorded at the chart speed of 20 mm/hour with the Bobrov type magnetometers. The variations were recorded in different time windows simultaneously by individual profiles. At each specific profile 10 - 15 field stations were run either on national basis or in co-operation with Polish and Slovak colleagues within the years between 1973-1990. Assuming the complex form of the Wiese relation between the two complex horizontal components $H_x, H_y$ and the complex vertical component $H_z$ the data samples recorded during the field experiments were analysed in both frequency and time domains to estimate different types of transfer functions (GTFs) and related induction response characteristics (in-phase and out-of-phase induction vectors) for

periods ranging from about 1000 to 7000 s. In our further analysis the single-station GTFs were used to generate anomalous magnetic fields and equivalent internal current systems.

## 3 Calculation and analysis of anomalous magnetic field using single-station transfer functions

To obtain a closer insight into the internal sources and the character of the anomalous induction, we applied the approach of Hypothetical Event Analysis (HEA) suggested in paper by Bailey et al. (1974), and developed further in Banks and Beamish (1984), and Banks (1986). There are two approaches we use in below.

### a) Hypothetical event analysis (HEA)

***No anomalous response in horizontal field is assumed.*** Applying a hypothetical uniform external inducing field of a specified amplitude and azimuth, and varying its azimuth to find the configuration that pick out the zones of anomalous induction most clearly, we generated and contoured the distribution of the anomalous magnetic field across the area covered by the single-station GTFs estimates,

$$H_x = H_x^0 = 1 \times \cos\Theta^0, \quad H_y = H_y^0 = 1 \times \sin\Theta^0, \quad H_z = A \times H_x^0 + B \times H_y^0.$$

The results of this approach are displayed in the set of contour maps in Fig. 3.

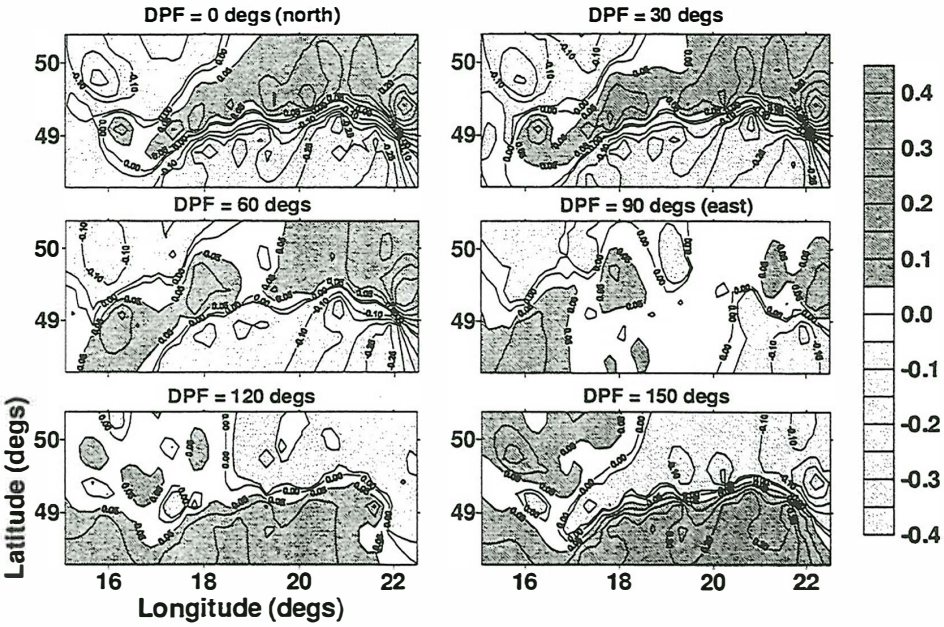


**Figure 3:** Contour maps of anomalous vertical magnetic field component (in A/km) generated by primary inducing field of unit module across the array of 150 sites with single-station GTFs estimates for the variation period of 96 min. Varying azimuths of the linearly polarised inducing field are shown by labels.

### b) Separation of the external and internal magnetic fields

***The horizontal magnetic field has both the external (regional) and internal (anomalous) parts.*** Using 3-D Hilbert Transform analogy we obtain the following relations between the magnetic field components in the non-conductive air,

$$H_x(x_0, y_0) = 2H_x^e + \frac{1}{2\pi} \int_{-\infty}^{\infty} \int_{-\infty}^{\infty} \frac{(x - x_0) H_z(x, y)}{\left[(x - x_0)^2 + (y - y_0)^2\right]^{3/2}} dx\, dy,$$

$$H_y(x_0,y_0) = 2H_y^e + \frac{1}{2\pi}\int_{-\infty}^{\infty}\int_{-\infty}^{\infty}\frac{(y-y_0)H_z(x,y)}{\left[(x-x_0)^2+(y-y_0)^2\right]^{3/2}}\,dx\,dy,$$

$$H_x^e = 1\times\cos\Theta^0, \qquad H_y^e = 1\times\sin\Theta^0, \qquad H_z = A\times H_x + B\times H_y.$$

With known GFTs, $A$ and $B$, the above formulae can be considered a coupled system of integral equations for the horizontal magnetic components if the primary external field is given. Solving these equations, either in the space or in the wave number domain, the HEA can be refined to give both anomalous vertical and anomalous horizontal magnetic fields for various azimuths of the primary external field.

Analysing the results of this refined approach, we conclude that practically the same distribution of the vertical component is generated as that in HEA approach. In principle, the most prominent induction pattern is expected to be obtained in both these cases when the external inducing field is perpendicular to the strike of an anomalous zone and the currents flow is parallel to its strike. We can see in a series of contour maps in Fig. 3 that both anomalous zones are well defined when the azimuths of the regional field are between 30 and 60°, and further for azimuth of 150°, corresponding approximately to NNE and SSE orientation of the regional field, respectively. The NNE azimuth, however, is practically parallel to the strike of the anomalous zone in the eastern margin of the BM. Both azimuths seem to suggest a strong influence of a conducting structure elongated in E-W direction, and of additional current distortions by 3-D structures.

The refined approach makes it possible to simulate not only the vertical field, but in addition also the horizontal GTFs and corresponding arrows. Relating difference fields between results of the refined and HEA approaches to normal horizontal components according to formulae

$$H_x^S - H_x^{HEA} = T_{xx}H_x^{HEA} + T_{xy}H_y^{HEA},$$
$$H_y^S - H_y^{HEA} = T_{yx}H_x^{HEA} + T_{yy}H_y^{HEA},$$

we estimate the complex elements $T_{ij}$. As the imaginary parts are very small, we define the arrows of only real parts, $\mathbf{T}_x = (\mathrm{Re}\,T_{xx}, \mathrm{Re}\,T_{yx})$ for the north, and $\mathbf{T}_y = (\mathrm{Re}\,T_{xy}, \mathrm{Re}\,T_{yy})$ for the east oriented primary fields. The results displayed in Fig. 4 show that the north oriented field, and corresponding E-W currents, generate a substantial anomalous part of the field evidenced by maximum arrows on the axis of the WCA zone. Also the BMA pattern seems to be evident. For the east oriented field, the WCA zone almost dissapears, while the BMA zone remains

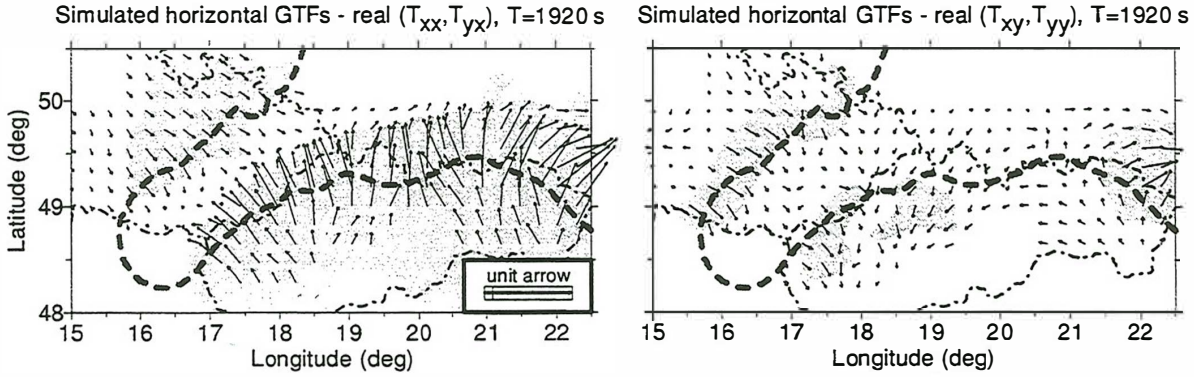


**Figure 4:** Distribution of vectors corresponding to real parts of simulated horizontal GTFs, T= 1920 s. **Left:** north oriented primary magnetic field (components $T_{xx}, T_{yx}$). **Right:** east oriented primary magnetic field (components $T_{xy}, T_{yy}$). Shaded area marks regions with arrows with magnitudes > 0.1.

clearly present across a slightly changed area. The magnitudes and spatial distribution of arrows remain essentially unchanged and, thus, independent of the direction of external inducing field. In this way, the different character of both anomalous zones is further evidenced. Clear 2-D character of the WCA anomaly is supported by imaging anomalous horizontal fields, while source and process of the BMA belt seems to be connected with distortion of currents by a conductor unknown as yet. With the seemingly paradoxical situations, when a quasi-linear anomaly is best excited by transversal currents, the question arises of possible large-scale static distortions of the geomagnetic transfer functions in the area involved. We will devote the next section to the analysis of this possibility.

**c) Estimation of the static-distortion effects**

A near-surface conductor, which is much smaller than the skin depth corresponding to the range of periods under investigation, can cause a spatial deviation of uniform regional currents through this local anomaly that generates anomalous magnetic field $\mathbf{B}^a$. Following the approach suggested in Ritter (1996), the local superposition of an anomalous field on the regional magnetic field $\mathbf{B}^0$ causes magnetic distortion

$$\mathbf{B}^a = \mathbf{D} \cdot \mathbf{E}^0 = \mathbf{D}.\mathbf{Z}^0 \cdot \mathbf{B}^0 .$$

For the vertical component, we then have

$$B_z^a = \left(D_{zx}, D_{zy}\right)\mathbf{Z}^0 \begin{pmatrix} B_x^0 \\ B_y^0 \end{pmatrix},$$

where $D_{zx}, D_{zy}$ are the vertical components of the magnetic distortion tensor (real and frequency independent ) and $\mathbf{Z}^0$ is the regional impedance tensor (contains complex phase information). Single-station GTFs can be expressed by following relation:

$$(A,B) = \left(A^0, B^0\right) + \left(A^a, B^a\right), \quad \left(A^a, B^a\right) = \left(D_{zx}, D_{zy}\right)\mathbf{Z}^0$$

When the anomalous magnetic field is assumed to have a unit amplitude and azimuth $\Theta^*$, the predicted magnetic field

$$B_z^p = \left[\left(A^0, B^0\right) + \left(D_{zx}, D_{zy}\right)\mathbf{Z}^0 \begin{pmatrix} 1 \cdot \cos\Theta^* \\ 1 \cdot \sin\Theta^* \end{pmatrix}\right]$$

Real and imaginary parts of $B_z^p$ for all sites, representing the same regional structure can be plotted in diagrams in the complex plane (Fig. 5), and then the data can be examined by gradually varying the angle $\Theta^*$.

When the regional structure is 1-D, the data in such diagrams arrange well along the line through the origin which indicates the phase of the regional impedance. The slope of this line does not depend on changes in the azimuth of the hypothetical variation event.

If the regional structure is 2-D, the distribution of the values in the complex plane is highly dependent on the azimuth $\Theta^*$. The data tend to cumulate closely along a line at a hypothetical field azimuth parallel to the regional strike direction, and at the perpendicular direction as well. The slope of this line indicates the phase angle of one of the regional impedances.

Analysing in this way the complex diagrams for the anomaly at the eastern margin of the BM, we do not obtain any clearly visible linear pattern for the most of the data, except the longest period available. For the period of 96 minutes, the points seem to arrange along a stright line for the direction of the regional field of about 60° (Fig. 5). For the perpendicular direction of this primary field, however, the data do not fall on a line, and cluster in a rather inorganized way. Thus, we can conclude that either the distortion model is inapplicable at all

in the specific conditions of the BMA, or that a considerable part of the observed vertical magnetic field results from the 2-D regional field, which violates the assumptions of the procedure applied. Unfortunately, no data are available from the region immediately to the N of our region of interest, which could give better idea as to the large-scale current distortions.

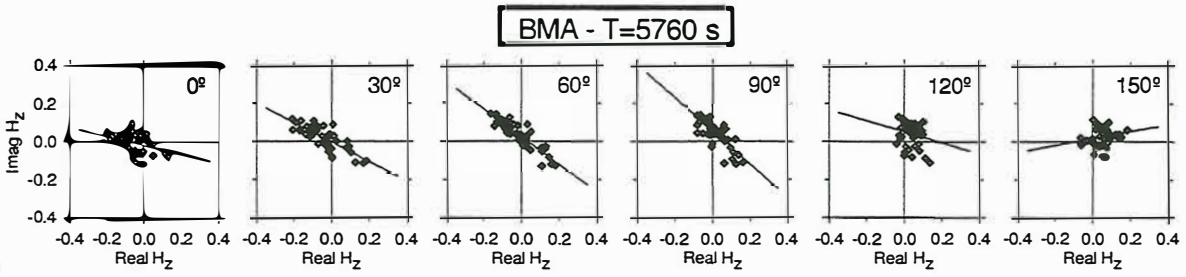


**Figure 5:** Diagrams of $ReH_z$ versus $ImH_z$ for different orientations of the primary inducing field and the period of 96 min. The data set was restricted to only the eastern margin of the BM. The negative slopes of diagrams are due to the reverse sign convention for the imaginary GTFs.

## 4 Equivalent current systems in a thin sheet at different depths

A thin sheet approximation can be applied when the long period variations are analysed (pseudo-stationary approach, $\omega \to 0$). In this case, the geomagnetic induction anomaly source is replaced by an equivalent current system in a thin sheet at a specified depth. In the unimodal case, the conductivity of the host medium is neglected, in the bimodal case the thin sheet is surrounded by a medium with a finite resistivity and can exchange currents with it.

The magnetic field at a point $P_0(x_0, y_0, z_0 = 0)$ on the earth's surface, produced by the current element with co-ordinates $(x, y, z)$ in a current sheet, can be written down using the Biot-Savart Law ( Banks, 1979)

$$\delta H_z(\mathbf{r}_0) = \frac{(x - x_0)J_y(\mathbf{r}) - (y - y_0)J_x(\mathbf{r})}{\left[(x - x_0)^2 + (y - y_0)^2 + z^2\right]^{3/2}} dx\, dy$$

where $J_x, J_y$ are the current density components that can be expressed as derivatives of the current stream function $\psi$ : $J_x(\mathbf{r}) = -\frac{\partial \psi(\mathbf{r})}{\partial y}$, $J_y(\mathbf{r}) = \frac{\partial \psi(\mathbf{r})}{\partial x}$.

The vertical current density $J_z(\mathbf{r})$ in this thin sheet model is constrained to be zero. Then the 2-D Fourier Transform is applied and the equation is inverted to express the current stream function:

$$\tilde{\psi}(\mathbf{k}, z) = -\frac{\exp(2\pi|\mathbf{k}|z)}{\pi|\mathbf{k}|}\tilde{H}_z$$

Following the method designed by Wang (1987) for taking into account effect of a conductive layered Earth, still under the assumption of the unimodal induction, we could further partly consider the influence of the conductive host medium on the current functions. For resistivities of the host medium of the order of thousends of Ωm, corrections to the empty-space sheet currents are, however, practically negligible.

## 5 Equivalent current systems for the eastern margin of the Bohemian Massif

Procedures described above suggest a practical method for generating maps of the equivalent current stream functions at different depths. Smooth configuration of the current function contours can be obtained only for depths above the current sheet. If the depth exceeds the anomalous current source depth, instabilities appear in current function distribution in virtue of continuing the field beyond the source top level. This process is demonstrated in Fig. 6 for the source depths of 10 km and 20 km. From the previous geophysical and geological data the internal source of the anomalous field at the eastern margin of the Bohemian massif is expected to be within the depths from about 10 km to 25 km. Having generated equivalent systems corresponding to NE orientation (60°) of inducing field for a series of different current sheet depths, the source depth is concluded to be about 18 km in the WCP region and about 10-12 km in the BM/BV region. These estimates are suggesting the anomaly sources in average at shallower depths than those obtained previously (16-26 km in the WCP region, (Jankowski et al., 1985), and 18-23 km at the eastern margin of the BM, (Pěčová and Praus, 1996) by separating the magnetic field into internal and external parts and applying the line current approximation). Both results are not controversial anyway, as line current approximation gives the maximum source depths.

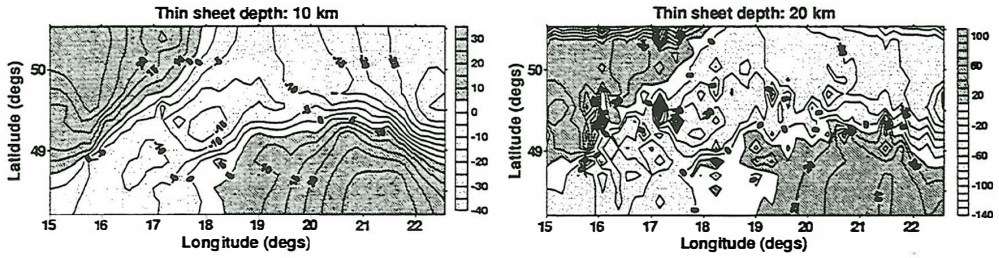


**Figure 6:** Current stream functions (units A/km) for the period of 32 minutes for a thin-sheet embedded at the depths of 10 and 20 km in a surrounding medium with conductivity of 0.001 S/m. Azimuths of the primary field is N60°E.

## 6 Conclusions

- The induction response data across the target area clearly indicate two anomalous zones - the West Carpathian Anomaly (WCA) of a 2-D character, which can be interpreted as a linear conductor extending along and distinguishing the whole Carpathian lithospheric plate, and a more complicated 3-D anomaly over the eastern margin of the Bohemian Massif (BMA). This picture does not principally change even after subtracting estimated effects of both the shallow conductive zones, assessed from the conductance maps across a broader region, and deep conductors at presumably asthenospheric depths, indicating thus pronounced crustal anomalies to be responsible for the observed induction pattern.
- Contour maps of the Central European induction data suggest a close connection of the BMA and WCP anomalous zones with those distinguishing the Trans-European Suture Zone extending across the Northern Germany and Poland (Červ et al., 1997).
- Analysing the vertical magnetic field distribution calculated from single-station transfer functions by two approaches, we find the best response for the perpendicular azimuth of the external field in the WCP anomalous zone - N-orientation for the central part of WCA, NNE orientation for its eastern part and SSE orientation for its western part - when the currents flow along the axis of the anomaly. On the contrary, for the BMA the best re-

sponse is seen for the external field quasi-parallel with the anomalous zone - for the N orientation in the northern part, and NNE to NEE orientation in its central and southern part.

- Contour maps of the internal vertical field component and equivalent current systems generated from the GTFs for varying azimuths of linearly polarised primary field seem to suggest a strong influence of E-W striking structures and subsequent current deflection by the 3-D structure of the region. Distribution of the equivalent current systems for a model of a thin sheet embedded in a two-layer medium indicate current flow concentration along both anomalies if the external inducing field is oriented perpendicular to the WCA strike and quasi-parallel to the BMA direction.
- The analysis of contour maps for current sheet depths between 10 and 20 km (Fig. 6) suggests an anomalous field source of the WCA at a depth of about 15-18 km, while the BMA source seems to be located shallower, at a depth of about 10 -12 km.
- From the equivalent internal current systems we can assume that in the case of BMA the anomalous internal fields are created by external source perpendicular to the anomalous zone. Two highly conducting zones seem to exist: in the SE (belongs to the Pannonian Basin) and in the NW, the latter being, however, not clearly attributable to the electrically anomalous regions known from the Central European region. The general trend of the regional field is then NW-SE and, on the eastern margin of the BM, a connection of the anomalous zones through a current channel seems to exist. BMA then seems to be a combined result of induction effects and current channelling. In correlation with deep geological structure this zone can delineate deep-seated boundary of two tectonic blocks with different geological history.

## References


Banks, R. J., 1979: The use of equivalent current systems in the interpretation of Geomagnetic Deep Sounding data. **56,** 139-157.

Bailey, R. C., Edwards, R. N., Garland, G. D., Kurtz, R., and Pitcher, D., 1974. Electrical conductivity studies over a tectonically active area in Eastern Canada. J. Geomagn. Geoelectr., **26,** 125-146

Červ, V., Pek, J., Praus O., 1984. Models of geoelectrical anomalies in Czechoslovakia. Journ. Geophys., **55 ,** 61 - 168.

Červ V., Pek J., Praus O., 1987: Numerical modelling of geoelectrical structure in Czechoslovakia. Phys. Earth Planet. Inter., **45**, 170-178.

Červ, V., Kováčiková, S., Pek, J., Pěčová, J., Praus, O.,1997. Model of Electrical Conductivity Distribution across Central Europe. J. Geomag. Geoelctr. ,**49**, 1585-1600.

Dudek, A., 1980. The crystalline basement block of the Outer Carpathians in Moravia: Brunovistulicum. Rozpr. Čs. Akad. Věd, Ř. mat. přír. věd, Praha, **90**, 1-85.

Jankowski, J.,Tarlowski, Z., Praus, O., Pěčová, J., Petr, V., 1985. The results of deep geomagnetic soundings in the Carpathians. Geoph. J. Roy. astr. Soc., **80**, 561-574.

Mísař, Z., Dudek, A., Havlena, V., Weiss, J., 1983. Geologie ČSSR I, Český masív, SPN Praha, 11-23.

Pěčová, J., Petr, V., Praus O., 1976. Depth distribution of the electrical conductivity in Czechoslovakia from electromagnetic studies. In: Ádam A.(Ed) Geoelectric and Geothermal Studies. KAPG Geophys. Monograph, Akademiai Kiado, Budapest, pp. 517-537.

Pěčová, J., Praus, O., 1996. Anomalous induction zones in the Czech Republic in relation to large scale European anomalies. Studia geoph. et geodaet., **40**, 50 - 76.

Pícha, B., Červ, V., Pek, J.,1984: Magnetotelluric inversion along the Osvetimany - Brezova pod Bradlom profile. Stud. geophys. et geodaet., **28,** 110 - 112

Praus, O., Pěčová, J., 1991: Anomalous geomagnetic fields of internal origin in Czechoslovakia. Studia geoph. et geodaet., **35**, 81 - 89.

Ritter, P., 1996. Separation of Local and Regional Information in Geomagnetic Response Functions using Hypothetical Event Analysis. Ph.D.Thesis, University of Edinburgh, Dept. of Geol. and Geophzs., pp 1 - 168.

Suk, M., 1995. Regional geological division of the Bohemian Massif. Exploration Geophysics, Remote Sensing and Environment, II, No.2, 25-30 .

Weiss, J., 1977. Basis of the Moravian block in the structure of the East European platform. Folia Fac sci. nat. Univ. Purk. Brun. Geol., XVIII, 5-64 ( in Czech).

Zapletal, K.,1932. Geologie a petrografie země moravskoslezské - 280 s. Brno (in Czech).